Spin soliton in a π-conjugated ladder polydiacetylene

Tadaaki Ikoma,* Shuji Okada, Hachiro Nakanishi, Kimio Akiyama, and Shozo Tero-Kubota
Institute of Multidisciplinary Research for Advanced Materials, Tohoku University, Sendai 980-8577, Japan

Klaus Möbius and Stefan Weber
Institute of Experimental Physics, Free University of Berlin, 14195 Berlin, Germany
(Received 26 November 2001; revised manuscript received 27 February 2002; published 12 July 2002)

The electronic structure and the spin dynamics of a spin soliton observed in a ''ladder''-structured polydiacetylene have been investigated using multifrequency pulsed and continuous-wave (cw) electron paramagnetic resonance (EPR), electron spin echo (ESE) spectroscopy, electron-nuclear double resonance (ENDOR), and electron-nuclear-nuclear triple resonance (TRIPLE). The undoped ladder polymer in which two polydiacetylene wires are linked by bridges consisting of two triple bonds exhibits a strong EPR signal. In contrast, no EPR signal is observed in the ladder-structured polydiacetylene, where the bridges consist of single bonds. The observed bridge effect on the probability of formation of paramagnetic centers is interpreted in terms of a quasidegenerate ground state due to the π-conjugated ladder structure that creates a π-bond kink corresponding to a spin soliton. High-frequency and high-field EPR reveals a small anisotropy of the g tensor (principal values $g_1=2.0037$, $g_2=2.0028$, and $g_3=2.0023$) for the spin soliton. By nutation spectroscopy, the spin multiplicity was confirmed to be $S=1/2$. The hyperfine pattern attributed to the β protons was detected by ENDOR and TRIPLE methods, providing evidence for both the positive and negative spin densities of the soliton wave function. These experimental results led to the conclusion that the unpaired electron of the spin soliton was substantially delocalized over the two polydiacetylenes through the π-conjugation. At temperatures (T) below 50 K, the width of the EPR spectrum narrows by about 45% with increasing temperature and the width remains nearly constant for $T>50$ K. The pronounced change in the line width for $T<50$ K suggests the presence of a mobile spin soliton in the ladder-structured polydiacetylene. A temperature dependence of the electron spin system's phase memory time T_M for $T<50$ K was also observed by ESE spectroscopy. The decay of the ESE exhibits a nonexponential behavior, with T_M increasing monotonically with rising temperature. These findings represent clear experimental evidence for motional narrowing phenomena. Based on a one-dimensional random-walk model for the unpaired electron spin along the ladder polymer, the soliton's diffusion rate constant was estimated from an analysis of the ESE dephasing process. An Arrhenius plot of the diffusion rate was asymptotic to $\approx 8\times 10^7$ s^{-1} at very low temperature, which is two orders of magnitude slower than that of the soliton in *trans*-polyacetylene.

DOI: 10.1103/PhysRevB.66.014423 PACS number(s): 75.60.Ch, 76.30.Mi, 76.70.Dx

I. INTRODUCTION

The existence of spin solitons is well established for both the *cis*- and *trans*-polyacetylenes. Over the past few decades, numerous theoretical and experimental studies on spin solitons in polyacetylenes have been presented in order to understand their nature as an elementary excitation in π-conjugated polymers.[1–8] In such systems, two different chemical structures with respect to the exchange of single and double bonds can be present in a single polyacetylene wire. These two different domains result in a degenerate ground state. In this framework, the soliton is defined as a domain wall separating the different structures and giving rise to an unpaired π-electron spin (without charge) at the position of the bond alternation kink.[1–3] However, the unpaired spin—or, in other words, the soliton wave function—is not localized at the specific carbon position corresponding to the kink, but rather is extended over several tens of carbon atoms[4,5,9–18] in balance with the localization and condensation energies.[4–6] Theoretically the spin soliton is able to move within the polymer wire by electron-phonon coupling.[4,5,19–22] The soliton's mobility has been demonstrated by various types of magnetic resonance experiments.[23–25] On the basis of the diffuse-trap model, in which the soliton visits some trapping sites and resides there for a long time compared to normal sites,[26–28] a comprehensive interpretation of the experimental data concerned with soliton dynamics confirms a one-dimensional soliton diffusion.[29,30]

A spin soliton is not observed in polydiacetylene wires with an alternating arrangement of double and single bonds. One reason for this may be the large energy gap between the domain with ene/yne structures and the domain with butatriene bonds. However, we have recently reported an intense electron paramagnetic resonance (EPR) signal due to a stable magnetic center in an undoped ladder polydiacetylene that was synthesized by the topochemical solid-state polymerization of a monomer crystal.[31,32] The polymer, denoted by LPDAT hereafter, is composed of two polydiacetylene wires which are regularly connected by bridges consisting of linked triple bonds (Fig. 1). The X band EPR spectrum of LPDAT consists of a single unstructured line at a resonance position corresponding to $g = 2.0030\pm 0.0005$. The spin concentration of the stable magnetic center in LPDAT is estimated to 4.6×10^{18} spin/g corresponding to the spin density of one unpaired electron in 240 monomer units. The ob-

 ©2002 The American Physical Society

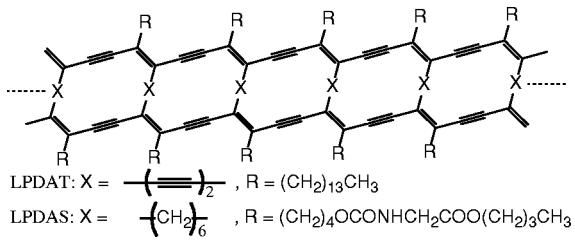

FIG. 1. Molecular structures of the ladder polymers of LPDAT and LPDAS.

served spectrum is quite different than those of various reactive intermediates such as biradicals and carbenes.[33] No changes in the EPR line shape and intensity of LPDAT have been observed over a time period of several years when the sample is stored at ambient temperature. Based on our previous results from electron spin echo envelope modulation (ESEEM) experiments, it was concluded that, similar to the spin soliton in polyacetylene, the unpaired electron spin of the stable magnetic center in LPDAT is delocalized over several units of the π-conjugated system.

In this contribution, we have utilized various magnetic resonance techniques, such as multifrequency EPR and pulsed electron-nuclear double and triple resonance (ENDOR and TRIPLE), to prove the existence of a spin soliton in LPDAT and to investigate its spin dynamics and electronic structure. In particular, EPR experiments performed at high microwave frequencies and correspondingly high magnetic fields enhance the spectral resolution determined by the *g* anisotropy of the paramagnetic center or by the *g* value difference of different sites.[34] The direct observation of an EPR response signal in the time domain by pulse techniques provides useful information on the spin relaxation and spin multiplicity of the spin system.[35] By ENDOR spectroscopy, the hyperfine interaction of individual magnetic nuclei with the unpaired electron spin is detected even in the case of inhomogeneously broadened EPR lines.[36] The extension to pulsed ENDOR detection allows unwanted relaxation effects among different spin sublevels to be avoided.[37] In TRIPLE resonance, the effect of an excitation of two nuclear spin transitions on the magnitude of the EPR signal is monitored. From the characteristic change in signal intensity, compared with those of the ENDOR signals, the relative signs of the hyperfine couplings can be determined.[38,39] Additionally, TRIPLE experiments allow one to distinguish whether or not the ENDOR signals are connected within the same paramagnetic center.

II. EXPERIMENTAL SECTION

Ladder-structured polymers in which the two polydiacetylene backbones were linked by single or triple bonds, as illustrated in the previous section, were produced by solid-state polymerization. The polymerization reaction proceeds by a successive 1,4-addition between the neighboring monomers in the crystal.[31,40] The monomers for LPDAT and LPDAS were 15,17,19,21,23,25-tetracontahexayne and 5,7,15,17-docosatetraynylene bis(*N*-(butoxycarbonylmethyl)carbamate), respectively, which were also synthesized. The ladder-structured polymers were sealed in quartz tubes for the EPR experiments.

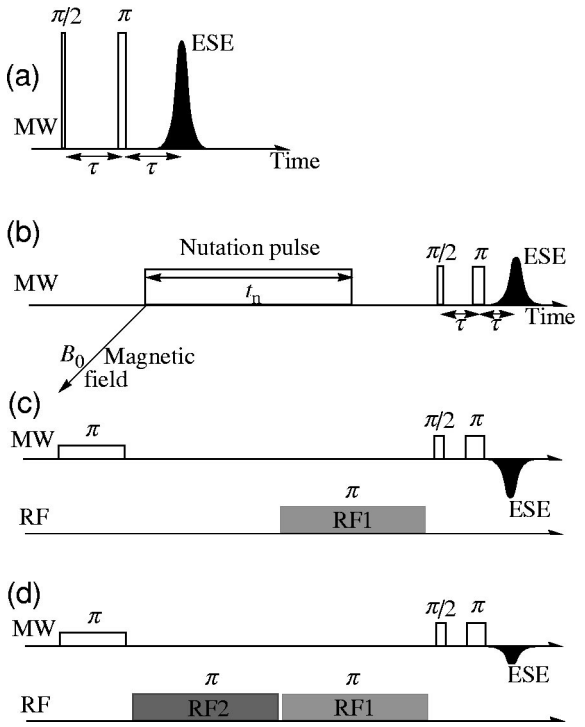

FIG. 2. Pulse schemes for (a) transverse spin relaxation, (b) 2D-nutation, (c) Davies-ENDOR, and (d) TRIPLE resonance experiments.

Multifrequency EPR experiments were performed at *S* (3.0 GHz), *X* (9.6 GHz), and *Q* (34.1 GHz) band frequencies using commercially available spectrometers (Bruker ESP-300 and ESP-380E). Continuous-wave (cw) EPR spectra of the *W* band were recorded with a laboratory-built high-field and high-frequency EPR spectrometer operating at 94–96 GHz.[41] The six-line EPR signal of a Mn(II)/MgO standard ($g=2.00101$, $|a|=8.71$ mT), placed near the sample in the cylindrical TE_{011} cavity, was simultaneously recorded for the *g*-factor calibration. Pulsed EPR, ENDOR, and TRIPLE experiments were performed at *X* band frequencies using the instrumentation equipped with a 1-kW traveling-wave tube (TWT) amplifier and an overcoupled dielectric resonator (Bruker ER4118X-W1), which was immersed in a helium gas flow cryostat (Oxford CF935). Radio-frequency (RF) pulses for the ENDOR and TRIPLE were generated with an RF synthesizer and amplified by a 1-kW TWT amplifier (Kalmus 166LPL). Unwanted signals within the detection time period were eliminated by a suitable set of phase cycles.

Figure 2 depicts the microwave (MW) and RF pulse sequences used in the pulsed multiresonance EPR studies. In all the experiments, a two-pulse electron spin echo (ESE) was used to observe the amplitude of the electron spin's longitudinal magnetization. A boxcar integrator was utilized to detect the total ESE intensity. As shown in Fig. 2(a), to observe the spin dephasing process of the spin system's transverse magnetization, the ESE intensity was monitored as a function of the pulse separation τ between the first and second MW pulses. For the nutation experiments [Fig. 2(b)],[42]

the ESE intensity derived from the last two MW pulses [duration: 48 ns ($\pi/2$ pulse) and 96 ns (π pulse)] was recorded as a function of the pulse length t_n of the preceding nutation pulse. The ESE intensity as a function of t_n was converted into the frequency domain by Fourier transformation. As the soft $\pi/2$ and π pulses selectively excite only a fraction of the inhomogeneously broadened EPR spectrum, two-dimensional (2D) nutation spectra were additionally obtained by observation of the t_n-dependent ESE oscillations as a function of the external magnetic field B_0. Two pulse schemes are commonly used in pulsed ENDOR spectroscopy, the Mims and the Davies pulse sequences.[37] We preferred the Davies ENDOR [Fig. 2(c)] over the Mims ENDOR, because blind spot effects in the Mims ENDOR may result in severely distorted ENDOR spectra which make it difficult to analyze the powder pattern spectrum. The Davies ENDOR pulse scheme utilized in this study consisted of a selective MW preparation pulse of duration 400 ns, followed by a RF pulse (RF1, 9.5 μs) that corresponds to a π pulse to excite the nuclear magnetic resonance (NMR). An ESE detection scheme, utilizing soft 96 and 200 ns MW pulses, follows the RF1 pulse to detect the hole depth in the inhomogeneous EPR line generated by the preparation pulse. To obtain the ENDOR spectrum, the ESE intensity was measured as a function of the frequency ν_{RF1} of the RF1 pulse. In the pulsed TRIPLE resonance, two RF pulses are applied between the MW preparation pulse and the ESE detection pulse sequence [Fig. 2(d)].[43] The frequency of RF2 (ν_{RF2}) is fixed at the resonance frequency for a selected NMR transition while the ESE intensity is measured as a function of the frequency of the RF1 pulse, ν_{RF1}. The TRIPLE effect (the difference TRIPLE spectrum) is obtained by subtracting the ENDOR spectrum, which was obtained from the pulse scheme without RF2, from the TRIPLE resonance data.

III. RESULTS

A. Multifrequency EPR

Figure 3 shows the cw EPR spectra of LPDAT and LPDAS observed at the *X* band at room temperature. An unstructured signal with a line width of 0.45 mT [full width at half maximum (FWHM)] is detected for LPDAT [Fig. 3(a)], whereas no EPR signal is observed for LPDAS. This is clear evidence that the π-conjugated bridging between the polydiacetylene wires plays an essential role in the occurrence of stable paramagnetic centers in polydiacetylene.

The spectral width (Δ_S) of an inhomogeneously broadened EPR line of a doublet radical may be decomposed into contributions arising from the anisotropic Zeeman interaction and unresolved hyperfine interactions:

$$\Delta_S = \frac{\Delta g}{g_e} h \nu_{MW} + \sum_i \Delta A_i . \quad (1)$$

Here, g_e is the g factor for a free electron, Δg represents the anisotropy of the g tensor, ΔA_i is the hyperfine coupling constants of magnetic nuclei (here ^{1}H and ^{13}C) interacting with the unpaired electron spin, and h is Planck's constant. While the contribution due to the anisotropic Zeeman interaction linearly depends on the magnetic field and, hence, on the MW frequency ν_{MW}, the linewidth contributions arising from hyperfine interactions are independent of ν_{MW}. The EPR spectral shape can be also influenced by a dynamic effect such as a random motion of the magnetic center with respect to the direction of the external magnetic field. However, the EPR measurement at higher ν_{MW} tends to freeze out the motional effect on the spectrum due to the shorter time scale for detection. Therefore, a multifrequency EPR study can be used to distinguish between the different contributions to the spectral broadening of the observed EPR line.

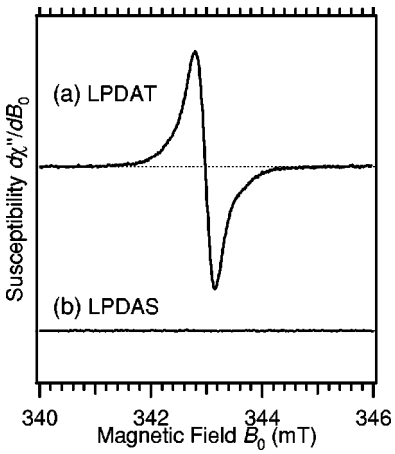

FIG. 3. cw EPR spectra of LPDAT and LPDAS observed at *X*-band frequency at room temperature. The amplitude and frequency of the field modulation for a phase-sensitive detection method were 0.1 mT and 100 KHz, respectively.

The cw EPR signal of LPDAT observed at different combinations of the magnetic field B_0 and microwave frequency is shown in Fig. 4. The signals taken at the *S* and *X* band frequencies are nearly symmetric and exhibit almost identical EPR linewidths. Therefore, we conclude that the signal linewidth at low frequencies is mainly determined by the unresolved hyperfine interactions. The spectra recorded at higher frequencies of the *Q* and *W* bands and correspondingly higher magnetic fields clearly reveal g anisotropies that manifest themselves in an increasing asymmetry of the LPDAT EPR signal. The simulation in a rigid-limit approximation of motion, which gives a powder pattern spectrum, reproduced well the observed spectrum at the *W* band using the principal g values of $g_1 = 2.0037 \pm 0.0001$, $g_2 = 2.0028 \pm 0.0001$, and $g_3 = 2.0023 \pm 0.000\,05$. The spectra at lower frequencies should be influenced by both static and dynamic effects because there are mobile and immobile magnetic centers in LPDAT as described in a later section. However, it was impossible to distinguish their contributions in the low-frequency spectra because the g anisotropy is not so large in comparison with the hyperfine interactions. Tentatively, the same g values have been used to calculate the spectral line shapes observed at lower MW frequencies [Fig. 4, traces (a)–(c)]. Organic polymer often undergoes oxidation and addition reactions with atmospheric oxygen molecules that create oxygen-centered radicals for which higher g_{iso} values and larger g anisotropies would be expected. However, the small g anisotropy taken together with a g_{iso} of 2.0029 is

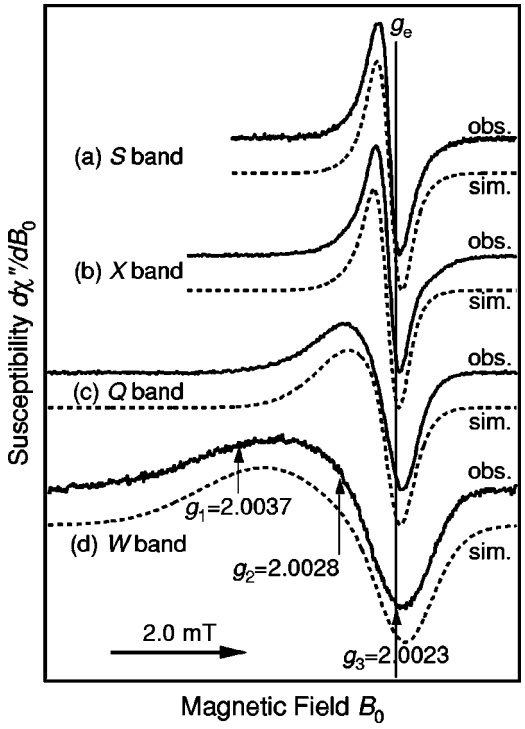

FIG. 4. cw EPR spectra of LPDAT observed at the microwave frequencies of (a) 2.9915 GHz, (b) 9.6130 GHz, (c) 34.059 GHz, and (d) 95.050 GHz at room temperature. The amplitude and frequency of the field modulation for a phase-sensitive detection method were 0.1 mT and 100 KHz, respectively. The dashed lines indicate the powder pattern spectra calculated using the orthorhombic principal g values (2.0023, 2.0028, and 2.0037) and anisotropic linewidths using Gaussian functions depending on the magnetic field.

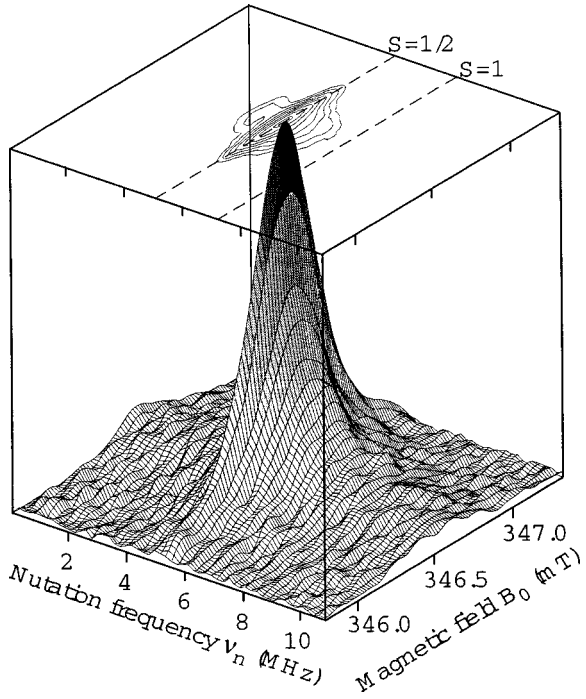

FIG. 5. 2D-nutation spectrum of LPDAT observed at the X band at room temperature.

characteristic for a carbon-centered radical in the π-conjugated polymer rather than for oxygen-centered radicals.

B. 2D-nutation spectroscopy

To confirm the effective spin multiplicity (S) of the stable magnetic center in LPDAT, transient nutation measurements were performed in two dimensions. For small MW irradiation fields (B_1), the nutation frequency (ν_n) for an EPR-allowed transition of $\Delta M_S = \pm 1$ can be expressed as[42,44–48]

$$\nu_n = \sqrt{S(S+1) - M_S(M_S-1)}\,\nu_1, \tag{2}$$

where ν_n is a critical function of S and M_S, and also depends on $\nu_1 = \gamma_e B_1$, and γ_e is the magnetogyric ratio for an electron spin. According to Eq. (2), the nutation frequency of a doublet state ($S = 1/2$) is expected to be smaller (by a factor of $\sqrt{2}$) than that of a triplet state ($S = 1$).

The 2D-nutation spectrum of LPDAT observed at the X band is depicted in Fig. 5. A strong signal is observed at a nutation frequency of 5.10 MHz centered at the resonance field of 346.5 mT. The same nutation frequency is observed in a calibration experiment with the organic radical of 2,2-diphenyl-1-picrylhydrazyl (DPPH) diluted in a KBr host crystal that is used as a standard for $S = 1/2$. Therefore, we concluded that the EPR signal has a doublet spin multiplicity. Thus, the stable magnetic center in LPDAT also behaves as a spin uncorrelated with the other unpaired electrons like the soliton in polyacetylene does.

C. ENDOR and TRIPLE resonance

The ESE-detected Davies-type ENDOR spectrum of LPDAT is depicted in Fig. 6(a). A broad and symmetric signal centered at the proton Larmor frequency of $\nu_H = 14.30$ MHz is observed. It is considered that these hyperfine signals almost stem from the pinned magnetic center since the motion of the center can be fast enough to average out the signals in the NMR frequency region of less than a few MHz. The main contributions to the ENDOR spectrum are expected to arise from the β protons within the alkyl side chain R ($-CH_2R'$). Because the hyperfine interaction of protons being more remote from the π-conjugated polydiacetylene wires quickly levels off with increasing distance, the very small couplings arising from the γ and δ protons are observed in a narrow region of the matrix line. The hyperfine interaction of the β protons is nearly isotropic and can be described by

$$A_\beta(\theta_i, \rho_i) = (A_0 + A_2 \sin\theta_i)\rho_i, \tag{3}$$

where the coefficient $A_2 = 164$ MHz reflects the spin density of a proton arising from hyperconjugation[49,50] and $A_0 = 0.8$ MHz contributions due to spin polarization.[51] ρ_i is the spin density on the polydiacetylene carbon C_i with the alkyl side chain and θ_i is the dihedral angle between the plane containing the C_i-C-H_β bonds and the principal direction of the p_z orbital of the C_i atom in which the unpaired electron spin resides. For $A_2 \gg A_0$, the size of the β proton hyperfine

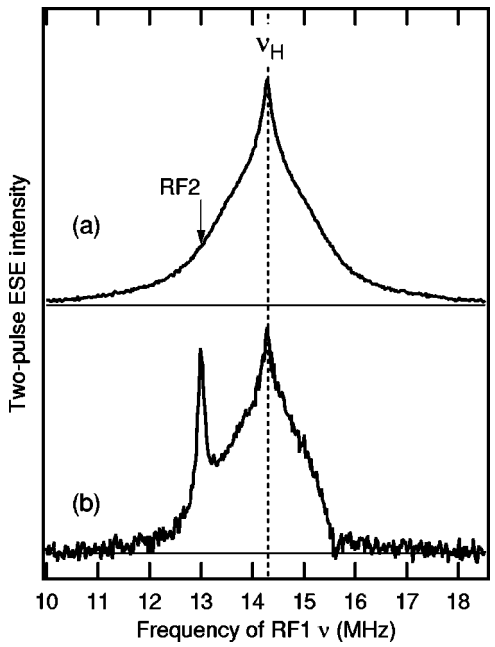

FIG. 6. (a) Davies-ENDOR spectrum for proton observed at room temperature. (b) Difference TRIPLE resonance spectrum obtained by pumping at 12.99 MHz.

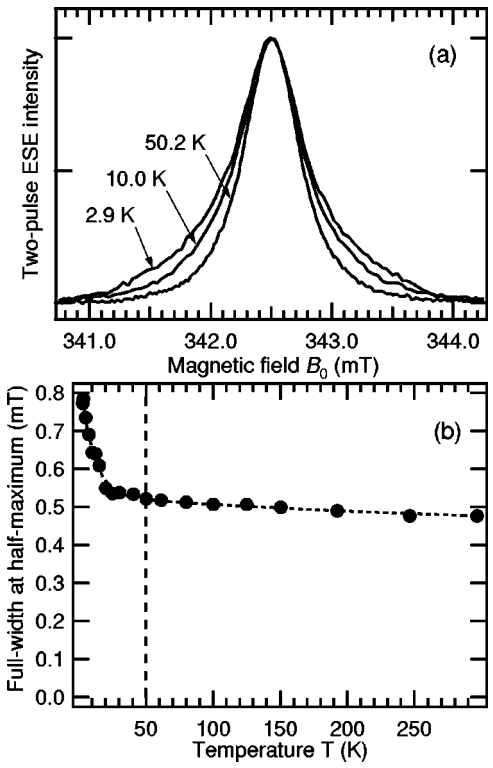

FIG. 7. Temperature dependence (a) of the two-pulse ESE detected EPR spectrum that is normalized at the top of the signal and (b) of the spectral linewidth. ESE was observed using $\pi/2$ (64 ns) and π (128 ns) pulses separated by 232 ns. The broken line through the data in b is a visual guide.

interaction critically depends on both the geometry of the alkyl side chain and the spin density on C_i. No well-resolved hyperfine lines arising from the β protons is a clear indication that a distribution of the spin density ρ_i and/or a distribution of geometric configurations is present, resulting in a broad and unresolved proton ENDOR spectrum.

The difference TRIPLE spectrum observed by pumping at 13.0 MHz is depicted in Fig. 6(b). TRIPLE resonance effects were observed in both regions lower and higher than ν_H. To excite the less hyperfine lines among the many signals included in the broad ENDOR spectrum, we chose the second RF frequencies that were as far from ν_H as possible. However, it was difficult to detect reliable difference TRIPLE signals when the frequency difference of $|\nu_{RF2}-\nu_H|$ became larger than 1.8 MHz due to the loss in signal intensity. The signal in the difference TRIPLE shows hyperfine lines correlated with the pumped line; i.e., they belong to the same spin center within the same M_S sublevel manifold. The conformational variation in the alkyl side chain never changes the sign of the proton hyperfine couplings. Therefore, the observation of difference TRIPLE signals on both sides of ν_H even during pumping the edge of the hyperfine spectrum suggests that negative as well as positive spin densities exist on the carbons bonding with the side chains.

D. Temperature dependence

Figure 7(a) depicts the temperature dependence of the ESE-detected *X* band EPR spectrum that was observed using two selective MW pulses. The spin center in LPDAT exhibits a symmetric EPR line with a FWHM of 0.775 mT at 2.9 K, which narrows by almost 45% when the temperature (T) is increased to 50 K. This behavior suggests that the mobility of the magnetic center affects the EPR spectral width. In Fig. 7(b), the FWHM of the EPR line is plotted as a function of the temperature. Line narrowing phenomena, as observed here for $T<50$ K, have been reported for the soliton in *trans*-polyacetylene which was found to be highly mobile along the π-conjugated wire of carbons.[2,3] For $T>50$ K, the nearly temperature-independent linewidth is similar to that of the soliton in *cis*-polyacetylene which was found to be immobilized. By comparison with the results observed for the soliton in polyacetylenes,[52–54] we conclude that the observed EPR line is composed of (a) contributions from mobile magnetic centers within the finite polymer chain length and (b) contributions of pinned centers that are trapped within the partially disordered regions of LPDAT.

Additionally, the temperature dependence of the ESE dephasing process has been studied (Fig. 8). While ESE dephasing proceeds efficiently at low temperatures, the process becomes slower and exhibits a nonexponential behavior as the temperature is increased. No MW power dependence on the ESE decay was observed, which is why instantaneous diffusion effects[55] can be ignored. The phase memory time lengthens by approximately 40% when the temperature is increased to 50 K. This corresponds to the decrease in the EPR linewidth observed in the same temperature range (see above). Therefore, we conclude that the ESE dephasing process (for $T<50$ K) arises from the diffusive motion of the magnetic center. On the other hand, the decay rate of the ESE becomes very fast again above 50 K. Such a behavior

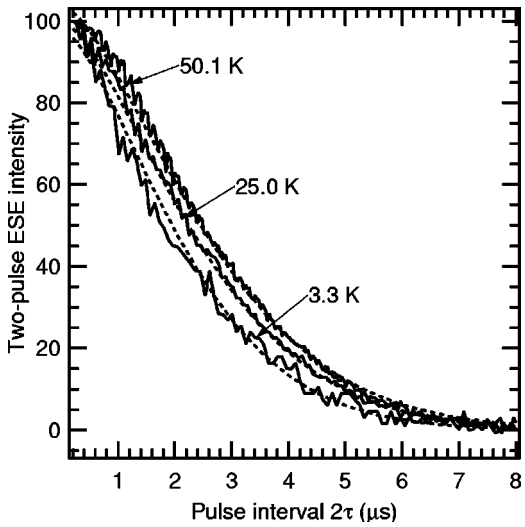

FIG. 8. Temperature dependence of two-pulse ESE decay observed by time increments (τ) between the first (16 ns) and second (32 ns) pulses. The ESE intensity is normalized at $2\tau = 200$ ns. The dashed lines describe the fitting curves.

implies that additional dephasing mechanisms, such as spin exchange, significantly contribute to the ESE decay at higher temperatures.

IV. DISCUSSION

A. Effect of conjugated bridges

Based on the characteristics, such as doublet spin multiplicity and delocalization of the electron spin and diffusive motion, the magnetic center observed in the undoped LPDAT where the two polydiacetylene wires are linked with π-conjugated bridges can be regarded as a spin soliton of the π-conjugated polymer. However, no soliton was observed in unbridged polydiacetylenes and in the respective LPDAS where the polydiacetylene wires were connected by aliphatic bridges. A soliton in a π-conjugated system can be defined as a π-bond kink between two domains with different chemical structures with respect to bond alternation within the polymer chain [Fig. 9(a)]. In the case of polydiacetylene, the π-bond structure in the one domain consists of a periodically repeating ene/yne unit, while in the other domain a butatriene structure is present. The conjugational defect at the junction between the two domains gives rise to an unpaired electron spin. In a single polydiacetylene wire, however, the two domains may not be simultaneously present within the same chain because the total energies for the two domains are very different [Fig. 9(b)]. In fact, in polydiacetylene, a periodic ene/yne structure has been confirmed from optical absorption spectroscopy and resonance Raman studies at temperatures below 300 K.[33,56] Therefore, a soliton is absent in the unbridged polydiacetylene.

When two polydiacetylenes are connected by bridges consisting of two consecutive triple bonds, the energies of the π orbitals are strongly affected by the conjugation effect between the two polymer wires. If the second polydiacetylene wire stabilizes the butatriene domain more than the ene/yne

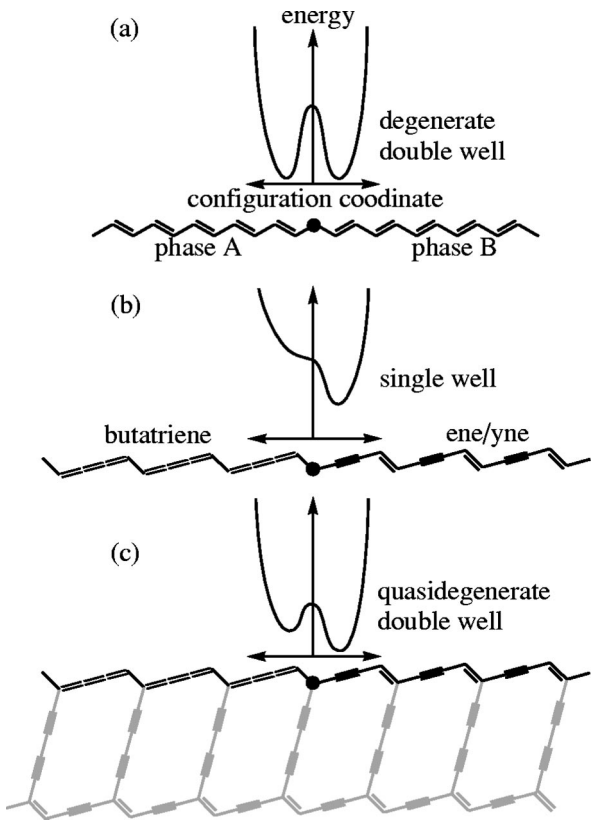

FIG. 9. Molecular structures and schematic potentials of (a) polyacetylene, (b) polydiacetylene, and (c) π-conjugated ladder polydiacetylene.

domain through the π-conjugated bridges, a pseudodegenerate ground state may be achieved [Fig. 9(c)]. As a consequence, this may lead to a soliton in LPDAT. Although the soliton in LPDAT does not have a mirror plane at the kink, as far as structural symmetry is concerned, such a situation is similar to the one present in *cis*-polyacetylene. On the other hand, the fact that no soliton is observed in LPDAS can be interpreted in terms of the aliphatic bridges not sufficiently assisting in stabilizing the conjugated π system to allow a butatriene domain to exist next to the ene/yne domain within the polydiacetylene wire.

B. Electronic structure

The deep nuclear modulation effect previously reported[32] and the small g anisotropy determined by multifrequency EPR indicate an electronic structure in which the unpaired electron spin is considerably delocalized within the π-conjugated system of carbons. Based on TRIPLE resonance, the broadening of the proton ENDOR signal can be mainly attributed to a distribution of the spin density on the carbons rather than a distribution of conformations of the alkyl side chains because they play an important role in the polymerization to fix the monomers at the proper positions in crystal by van der Waals forces. Therefore, the alkyl side chains in LPDAT tend to form a coplanar structure with the polymer sheet. The most probable conformation consequently results in $\theta_i = 30°$. Using this dihedral angle, the

observed main hyperfine signals within the range $\nu_H \pm 1.8$ MHz lead [according to Eq. (3)] to $|\rho| \leqslant 0.026$. Although the total spin distribution cannot be probed by ENDOR because of the lack of hyperfine information from carbons without attached alkyl side chains, the estimated small spin density on the specific carbon C_i is consistent with a considerable delocalization of the soliton's unpaired electron spin.

By TRIPLE resonance, the presence of a negative spin density was proved for the soliton in LPDAT. In the soliton of *trans*-polyacetylene, the positive spin density appears at every even-numbered carbon relative to the center of the soliton, reflecting the nonbonding character of the soliton whose energy is localized at the center of the band gap.[4,5] On the other hand, a negative spin density is induced at odd-numbered carbons by spin polarization due to the effect of electron correlation.[57] The negative spin density of LPDAT can be understood by the spin polarization effect at the odd-numbered carbon sites from the soliton center. Each carbon with an attached alkyl side chain on the polydiacetylene wire, where the spin center is located, corresponds to the odd-numbered carbon site. The carbons with the alkyl groups on another polydiacetylene wire give rise to the even numbered carbon sites. Hence, the occurrence of both positive and negative spin densities also suggests the effect of π-conjugation and the delocalization of the unpaired electron spin over two polydiacetylene wires.

C. Spin dynamics

The temperature dependences of both the EPR spectrum and the ESE dephasing process were observed for the soliton in LPDAT, indicating mobility. To estimate the diffusion rate of the soliton, we have analyzed the ESE decay with a model for a one-dimensional random-walk process.[58] Here, we assume that within an infinite polymer wire soliton, hopping takes place only between nearest-neighbor sites and that the hopping rate constant k_d is much larger than $1/t$. According to Kubo and Tomita's formalism,[59] the response function $S(t)$ is expressed as

$$S(t) = \exp\left[-\frac{\Delta\omega^2}{12\pi^2 k_d^2}\{(1+4\pi k_d t)^{3/2} - 6\pi k_d t - 1\}\right]. \tag{4}$$

Here $S(t)$ is an exponential function that decays with the characteristic $t^{3/2}$ and t dependences of its exponent. $\Delta\omega$ represents the local magnetic field that an unpaired electron spin experiences within one site, which is an ensemble average of the nuclear hyperfine couplings in the soliton. $\Delta\omega$ of the soliton in LPDAT can be estimated from an integration of the proton ENDOR spectrum, because the local magnetic field is almost exclusively governed by hyperfine interactions with the β protons of the alkyl side chains. The observed ESE decays in Fig. 8 are well fitted by a nonlinear least-squares method using the function $S(t)$ with $\Delta\omega = 2.5$ MHz.

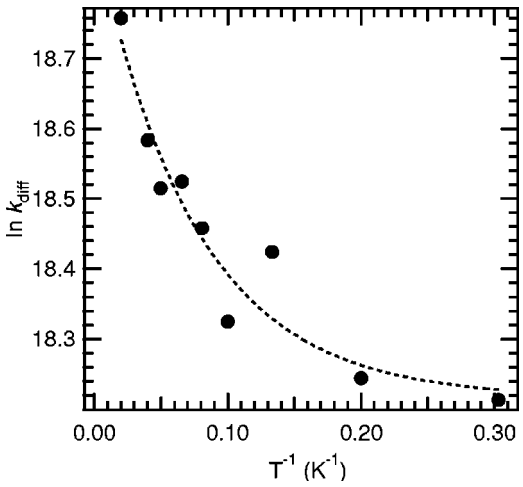

FIG. 10. Arrhenius plot for the diffusion rate constant (k_d) estimated from the dephasing curves of ESE. The dashed line drawn through the data can be used as a visual guide.

In Fig. 10, $\ln(k_d)$, which was obtained from the analysis of the ESE decay according to Eq. (4), is plotted versus the inverse temperature. The Arrhenius plot is asymptotic to $\approx 8\times 10^7$ s^{-1} at very low temperatures. This value is two orders of magnitude slower than the on-chain diffusion rate constant determined for the soliton in *trans*-polyacetylene.[29,30] The soliton center corresponding to the π-bond alternation kink can be displaced by the exchange of one of the single bonds with the adjacent multiple bonds, resulting in a displacement of the soliton. The relatively slow diffusion rate in LPDAT is probably associated with the exchange between the double and triple bonds or the imperfect degeneracy of the electronic energies for the ene/yne and butatriene domains. On the other hand, the diffusion rate is exponentially accelerated above 10 K. There seems to be some small barrier of local potential for the soliton, which is necessary for a rearrangement of the π bonds. The driving force of the nonballistic soliton diffusion may be related to scattering with the low-frequency phonon.

V. CONCLUSION

Using various EPR methods, we have studied the electronic structure and the dynamics of the stable magnetic center newly observed in the undoped ladder polydiacetylene that is regularly linked by π-conjugated triple bonds. Based on several spectroscopic features, it was concluded that the magnetic center is a spin soliton. The π-conjugation effect between two polydiacetylene wires on the spin soliton was examined by comparison with a ladder-structured polydiacetylene that is bridged by aliphatic bonds. It was considered that the π-conjugated ladder structure achieves a quasidegenerate ground state of the ene/yne and the butatriene domains, and this introduces the spin soliton in polydiacetylene. The results of multifrequency EPR and 2D-nutation measurements are indicative of the fact that

unpaired electrons with the doublet state are delocalized over the π-conjugated carbons. The ENDOR and TRIPLE resonance spectra due to the protons within the alkyl side chains confirm the presence of positive and negative spin densities in the soliton wave function and, furthermore, suggest the delocalization of the soliton over both polydiacetylene wires. The temperature dependences of the EPR spectral width and the ESE phase memory time, observed in the temperature region of 3 $K < T < 50$ K, indicate mobility of the spin soliton. The diffusion rate constants were estimated by employing a random-diffusion model in a one-dimensional polymer chain of infinite length. The intrinsic rate constant of the spin soliton in the ladder-structured polydiacetylene is slower than that observed in *trans*-polyacetylene having a completely degenerate ground state.

ACKNOWLEDGMENTS

Thanks are due to Dr. P. Höfer and Dr. A. Kamlowski (Bruker Analytik GMBH) for measurements of *W* band ENDOR and due to Dr. H. Matsuzawa (Tohoku University) for preparation of the LPDAS. T.I. is grateful to Professor S. Kuroda (Nagoya University) and Professor T. Ichikawa (Hokkaido University) for providing valuable preprints and comments. This research was funded in part by a Grant-in-Aid for Scientific Research (No. 12740310) from the Japan Ministry of Education, Science, Sports and Culture, by Izumi Science and Technology Foundation, and by the Deutsche Forschungsgemeinschaft (SFB-498-Teilprojekt A2- and SPP-1051 ''Hochfeld-EPR in Biologie, Chemie und Physik''), which are gratefully acknowledged.

*Electronic address: ikoma@tagen.tohoku.ac.jp; URL: http://www.icrs.tohoku.ac.jp/research/tero/index-e.html

[1] H. Shirakawa, T. Ito, and S. Ikeda, Macromol. Chem. **179**, 1565 (1978).
[2] I. B. Goldberg, H. R. Crowe, P. R. Newman, A. J. Heeger, and A. G. MacDiarmid, J. Chem. Phys. **70**, 1132 (1979).
[3] B. R. Weinberger, E. Ehrenfreund, A. Pron, A. J. Heeger, and A. G. MacDiarmid, J. Chem. Phys. **72**, 4749 (1980).
[4] W. P. Su, J. R. Schrieffer, and A. J. Heeger, Phys. Rev. Lett. **42**, 1698 (1979).
[5] W. P. Su, J. R. Schrieffer, and A. J. Heeger, Phys. Rev. B **22**, 2099 (1980).
[6] A. J. Heeger, S. Kivelson, J. R. Schrieffer, and W. P. Su, Rev. Mod. Phys. **60**, 781 (1988).
[7] S. Curran, A. Stark-Hauser, and S. Roth, in *Handbook of Organic Conductive Molecules and Polymers*, edited by H. S. Nalwa (Wiley, Chichester, 1997), Vol. 2, Chap. 1, p. 1.
[8] K. Mizoguchi and S. Kuroda, in *Handbook of Organic Conductive Molecules and Polymers* (Ref. 7), Vol. 3, Chap. 6, p. 251.
[9] H. Thomann, L. R. Dalton, Y. Tomkiewicz, N. S. Shiren, and T. C. Clarke, Phys. Rev. Lett. **50**, 533 (1983).
[10] L. R. Dalton, H. Thomann, A. Morrobel-Sosa, C. Chiu, M. E. Galvin, G. E. Wnek, Y. Tomkiewicz, N. S. Shiren, B. H. Robinson, and A. L. Kwiram, J. Appl. Phys. **54**, 5583 (1983).
[11] S. Kuroda, H. Bando, and H. Shirakawa, Solid State Commun. **52**, 893 (1984).
[12] S. Kuroda, H. Bando, and H. Shirakawa, J. Phys. Soc. Jpn. **54**, 3956 (1985).
[13] S. Kuroda and H. Shirakawa, Phys. Rev. B **35**, 9380 (1987).
[14] S. Kuroda and H. Shirakawa, Solid State Commun. **77**, 937 (1991).
[15] S. Kuroda and H. Shirakawa, J. Phys. Soc. Jpn. **61**, 2930 (1992).
[16] H. Käss, P. Höfer, A. Grupp, P. K. Kahol, R. Weizenhöfer, G. Wegner, and M. Mehring, Europhys. Lett. **4**, 947 (1987).
[17] M. Mehring, A. Grupp, P. Höfer, and H. Käss, Synth. Met. **28**, D399 (1989).
[18] P. K. Kahol and M. Mehring, J. Phys. C **19**, 1045 (1986).
[19] K. Maki, Phys. Rev. B **26**, 2181 (1982).
[20] K. Maki, Phys. Rev. B **26**, 2187 (1982).
[21] S. Jeyadev and E. M. Conwell, Phys. Rev. B **36**, 3284 (1987).
[22] Y. Wada, Prog. Theor. Phys. Suppl. **113**, 1 (1993).
[23] N. S. Shiren, Y. Tomkiewicz, T. G. Kazyaka, A. R. Taranko, H. Thomann, L. Dalton, and T. C. Clarke, Solid State Commun. **44**, 1157 (1982).
[24] J. Tang, C. P. Lin, M. K. Bowman, J. R. Norris, J. Isoya, and H. Shirakawa, Phys. Rev. B **28**, 2845 (1983).
[25] K. Mizoguchi, Jpn. J. Appl. Phys., Part 1 **34**, 1 (1995).
[26] M. Nechtschein, F. Devreux, R. L. Greene, T. C. Clarke, and G. B. Street, Phys. Rev. Lett. **44**, 356 (1980).
[27] K. Holczer, J. P. Boucher, F. Devreux, and M. Nechtschein, Phys. Rev. B **23**, 1051 (1981).
[28] M. Nechtschein, F. Devreux, F. Genoud, M. Guglielmi, and K. Holczer, Phys. Rev. B **27**, 61 (1983).
[29] K. Mizoguchi, K. Kume, and H. Shirakawa, Solid State Commun. **50**, 213 (1984).
[30] K. Mizoguchi, S. Masubuchi, K. Kume, K. Akagi, and H. Shirakawa, Phys. Rev. B **51**, 8864 (1995).
[31] S. Okada, K. Hayamizu, H. Matsuda, A. Masaki, N. Minami, and H. Nakanishi, Macromolecules **27**, 6259 (1994).
[32] T. Ikoma, S. Okada, H. Nakanishi, K. Akiyama, and S. Tero-Kubota, Solid State Commun. **117**, 285 (2001).
[33] H. Sixl, in *Advances in Polymer Science*, edited by H. J. Cantow and H. Joachim (Springer-Verlag, Berlin, 1984), Vol. 63, p. 49.
[34] K. Möbuis, in *Biological Magnetic Resonance*, edited by L. J. Berliner and J. Reuben (Plenum Press, New York, 1993), Vol. 13, Chap. 6, p. 253.
[35] A. Schweiger, Angew. Chem. Int. Ed. Engl. **30**, 265 (1991).
[36] S. Kuroda, Int. J. Mod. Phys. B **9**, 221 (1995).
[37] C. Gemperle and A. Schweiger, Chem. Rev. **91**, 1481 (1991).
[38] K. P. Dinse, R. Biehl, and K. Möbius, J. Chem. Phys. **61**, 4335 (1974).
[39] R. Biehl, M. Plato, and K. Möbius, J. Chem. Phys. **63**, 3515 (1975).
[40] H. Matsuzawa, S. Okada, A. Sarkar, H. Nakanishi, and H. Matsuda, J. Polym. Sci., Part A: Polym. Chem. **37**, 3537 (1999).
[41] T. F. Prisner, M. Rohrer, and K. Möbius, Appl. Magn. Reson. **7**, 167 (1994).
[42] T. Ikoma, O. Ito, S. Tero-Kubota, and K. Akiyama, Energy Fuels **12**, 996 (1998).
[43] M. Mehring, P. Höfer, and A. Grupp, Ber. Bunsenges. Phys. Chem. **91**, 1132 (1987).
[44] J. Isoya, H. Kanda, J. R. Norris, J. Tang, and M. K. Bowman, Phys. Rev. B **41**, 3905 (1990).

[45] A. V. Astashkin and A. Schweiger, Chem. Phys. Lett. **174**, 595 (1990).
[46] N. Mizuochi, Y. Ohba, and S. Yamauchi, J. Phys. Chem. A **101**, 5966 (1997).
[47] K. Sato, M. Yano, M. Furuichi, D. Shiomi, T. Takui, K. Abe, K. Itoh, A. Higuchi, K. Katsuma, and Y. Shirota, J. Am. Chem. Soc. **119**, 6607 (1997).
[48] T. Ikoma, O. Ito, and S. Tero-Kubota, Energy Fuels **16**, 40 (2002).
[49] C. Heller and H. M. McConnell, J. Phys. Chem. **32**, 1535 (1960).
[50] A. Horsfield, J. R. Morton, and D. H. Whiffen, Mol. Phys. **4**, 425 (1961).
[51] J. R. Bolton, A. Carrington, and A. D. McLachlan, Mol. Phys. **5**, 31 (1962).
[52] M. Mehring, H. Seidel, W. Müller, and G. Wegner, Solid State Commun. **45**, 1075 (1983).
[53] H. Thomann, H. Jin, and G. L. Baker, Phys. Rev. Lett. **59**, 509 (1987).
[54] E. J. Hustedt, H. Thomann, and B. H. Robinson, J. Chem. Phys. **92**, 978 (1990).
[55] J. R. Klauder and P. W. Anderson, Phys. Rev. **125**, 912 (1962).
[56] G. J. Exarhos, W.M. Risen, Jr., and R. H. Baughman, J. Am. Chem. Soc. **98**, 481 (1976).
[57] K. R. Subbaswamy and M. Grabowski, Phys. Rev. B **24**, 2168 (1981).
[58] J. Tang, S. N. Dikshit, and J. R. Norris, J. Chem. Phys. **103**, 2873 (1995).
[59] R. Kubo and K. Tomita, J. Phys. Soc. Jpn. **9**, 888 (1954).